The remote determination of magnetic remanence

David A. Pratt
Tensor Research
PO Box 8159
Greenwich NSW 2065
david.pratt@tensor-research.com.au

Keith Blair McKenzie
Tensor Research
PO Box 8159
Greenwich NSW 2065
blair.mckenzie@tensor-research.com.au

Anthony S. White
Tensor Research
PO Box 8159
Greenwich NSW 2065
tony.white@tensor-research.com.au

SUMMARY

The remote determination of magnetic remanence in rocks is a method that has largely been ignored because of the ambiguity associated with the estimation of both the Koenigsberger ratio and remanent magnetization direction. Our research shows that the resultant magnetization direction can be derived directly through inversion of magnetic data for an isolated magnetic anomaly. The resultant magnetization direction is a property of the target magnetic rocks and a robust inversion parameter. The departure angle of the resultant magnetization vector from that of the inducing magnetic field is an important indicator of the existence of remanent magnetization and the inversion process can detect departures that are not easily detected by visual inspection. This departure angle is called the Apparent Resultant Rotation Angle or ARRA.

The induced field vector, remanent magnetization vector and resultant magnetization vector lie on a great circle. We find the intersection of the polar wander vector trace with the great circle to obtain one or more possible solutions for the remanent magnetization direction. Geological deduction will normally allow us to reduce the ambiguity for multiple solutions to obtain the most likely remanent magnetization direction. Once the remanent magnetization direction is established, it is then possible to determine the Koenigsberger ratio and magnetic susceptibility for the target.

We illustrate the methodology with some synthetic models and targets from Australian magnetic surveys. Magnetic remanence is a physical property of the rock that is distinct from susceptibility and this methodology provides a new tool to help with the categorization and prioritization of exploration targets.

Key words: resultant, magnetization, remanence, susceptibility, inversion.

INTRODUCTION

The remote, quantitative estimation of magnetic remanence has long been regarded as a difficult if not impossible task for the interpretation of magnetic surveys. This impression has largely been shaped by early literature on the subject that focused on the use of semi-infinite models to demonstrate the inherent ambiguity between dip and magnetization direction (Grant and West, 1965). This ambiguity is significantly reduced once we use geophysical inversion of data for isolated magnetic anomalies.

We demonstrate three important ideas that allow us to estimate the remanent magnetic properties of a remote target and deliver new geological information about the target as well as reducing ambiguity in the interpretation.

1. Select only limited strike length magnetic anomalies for inversion.
2. Allow the resultant magnetization vector to be a variable in the inversion rather than the assumption of a pure, induced field. This vector combines both the inducing and remanent magnetization field components.
3. Find the intersection of the great circle plane defined by the local induced field vector and resultant magnetization vector with the polar wander magnetization direction at the target site.

We show experimental results for a range of models that demonstrate the robust nature of resultant magnetization vector inversion and then apply the methods to a field site with existing laboratory measurements of remanence and an untested site in the NSW, Thompson Fold Belt.

RESULTANT MAGNETIZATION INVERSION

While remanent magnetization is an intrinsic property of a geological unit, it is the resultant magnetization vector that determines the shape and amplitude of the measured magnetic anomaly over the target. Figure 1 shows examples of east west profiles across the intrusive magnetic pipe "D" from Figure 5 modelled with weak, strong and no remanence.

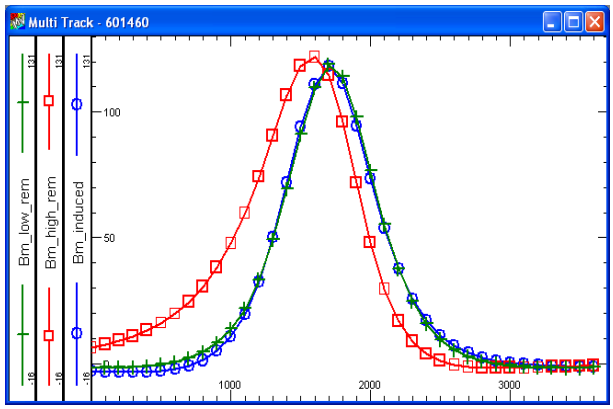

Figure 1. Example east west profiles over a vertical magnetic pipe (D) showing the results for induced magnetization (blue circles), weak remanence (green +) and strong remanence (red square).

While the difference between the weak remanence (green) and induced (blue) curves in Figure 1 is small for a single profile, inversion of all the surrounding lines makes it possible to see very small departures in the resultant magnetization vector. The ARRA angle for the weak and strong remanence cases is 24 degrees and 127 degrees respectively.

An important outcome of this observation is the fact that neither the magnetic susceptibility or Koenigsberger ratio is required for calculating the anomaly. Only the direction and amplitude of the resultant magnetization vector is required.

By inverting for the resultant magnetization vector rather than the assumed induced field vector, it is possible to resolve dip for isolated magnetic anomalies as well as the direction of the resultant magnetization vector. This outcome was implied by independent work done on the estimation of the resultant magnetization direction using magnetic moments by Schmidt and Clark (1998), Foss and McKenzie (2006), Caratori Tontini and Pedersen (2008), the virtual pole from magnetic anomaly (VPMA) method by Cordani and Shukowsy (2009) and the magnetic transform search method by McKenzie *et al* (2012). The magnetic moment and VPMA methods use deterministic procedures for calculation of the resultant magnetization vector direction. All three methods require removal of the regional magnetic field prior to the procedure because tilt in the residual field will influence the estimation of the resultant magnetization direction.

Theoretical examples of resultant inversion

We ran a number of experiments on theoretical models to test the premise that geometry and the resultant magnetization vector could be resolved without major ambiguity. We started with simple tests on azimuth, dip and Q variations for a dipping tabular body and then expanded the tests to include changes in the upper surface shape.

We used a tabular body model at a depth of 100 metres with Q values of 0.5 and 2.0 and seven dips ranging from 30 degrees to 150 degrees. Each tabular body had a width of 200 metres, strike length of 1000 metres and depth extent of 900 metres. Five percent RMS noise was added to the original simulated data. This exercise was repeated for the case where Q = 2.0, but an elliptical pipe was used to approximate the tabular body used to create the synthetic data. The results of these inversions are summarised in Table 1.

Table 1. Tabular body inversion results.

Parameter	Tabular Av. Error (14 models)	Elliptic Pipe Av. Error (7 models)
Dip	0.51 degrees	2.49 degrees
Azimuth	0.13 degrees	0.91 degrees
Depth	0.82 metres	9.43 metres
Resultant inclination	0.29 degrees	4.27 degrees
Resultant declination	0.46 degrees	6.65 degrees

There is a shape mismatch between the original tabular body and elliptic pipe at shallow dips that produces much larger errors than those for steep dips. This mismatch decreases as the depth to width ratio increase beyond 1.0. The resultant magnetization vector error for the vertical elliptic pipe in this test was 0.48 degrees for inclination and 0.70 degrees for the declination. This result is more relevant as steep dips or plunges are more likely for isolated intrusive targets.

The impact of map geometry

The next set of tests purposely applied an incorrect selection of the map shape geometry to a series of polygonal, vertical pipe like targets (Figure 2).

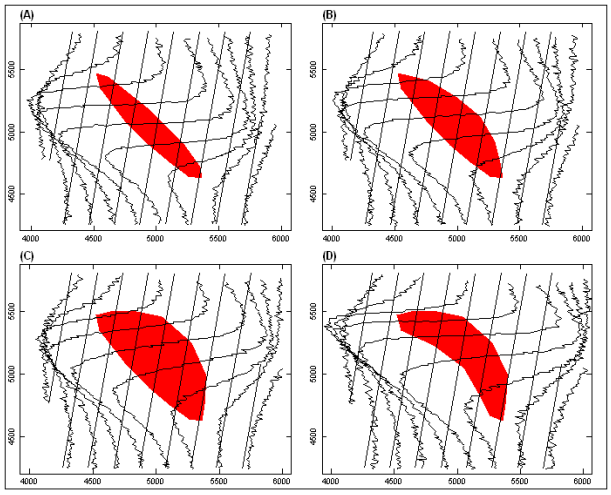

Figure 2. Example of the four shapes used to generate the target models for vertical magnetic pipes and the simulated data channels with 5% RMS noise added.

Table 2 list the results for the cases where the variable shape targets are buried at 200 metres below the sensor profiles using a tabular body and elliptical pipe shape to approximate the targets. Even though the elliptic pipe is a better shape to use, the results are very similar for the range of tests with the average error for resultant magnetization inclination and declination less than 1 degree.

Table 2. Variable map shape inversion results for 200m deep variable shape vertical polygonal targets (4 models).

Parameter	Tabular Av. Error	Elliptic Pipe Av. Error
Dip	2.03 degrees	2.78 degrees
Azimuth	0.80 degrees	0.92 degrees
Depth	6.25 metres	6.33 metres
Resultant inclination	0.51 degrees	0.64 degrees
Resultant declination	0.15 degrees	0.24 degrees

Table 3 lists a similar set of tests, except the target is at a depth of 100 metres. Again the results are very similar with the average errors for the resultant magnetization inclination and declination less than 1 degree.

Table 3. Variable map shape inversion results for 100m deep variable shape vertical polygonal targets (4 models).

Parameter	Tabular Av. Error	Elliptic Pipe Av. Error
Dip	2.38 degrees	2.70 degrees
Azimuth	0.93 degrees	0.98 degrees
Depth	10.68 metres	10.43metres
Resultant inclination	0.87 degrees	0.80 degrees
Resultant declination	0.46 degrees	0.38 degrees

As the target shallows, the error in the depth increases for a severe mismatch in the map shape of the target, but the resultant magnetization direction remains accurate.

These experiments demonstrate the robustness of inversion for the resultant magnetization direction along with the ability to resolve other target parameters such as shape azimuth and dip. This conclusion applies to discrete magnetic anomalies will degrade as the strike length of a target increases. The same limitations apply to the magnetic moment and VPMA methods.

RECOVERY OF REMANENT MAGNETIZATION

Once the resultant magnetization vector has been recovered by inversion of a specific target, the next step is to determine the remanent magnetic vector direction. We can assume that the induced field direction, resultant magnetization direction and the resultant magnetization amplitude are known, but Q and magnetic susceptibility are unknown. As Q is varied, the remanent vector will move along part of the great circle, but a value of Q is required to estimate the magnetic susceptibility of the target.

The apparent polar wander path (APWP) is established for most continents and this information can be used to calculate the remanent magnetic field vector as a function of geological time at the location of the target (Merrill, McElhinny and McFadden, 1996). We call this the transformed APWP or TAPWP. The vector defined by the TAPWP intersection with the great circle defined by inversion is the remanent magnetization vector direction of the target. This assertion assumes that there has been no drift in the remanent magnetization vector since the target was magnetized. Where multiple intersections exist, geological reasoning can be applied to determine the most probable intersection. We note that the valid range of the remanent magnetization vector is limited to a geometrically realisable subset of the great circle.

Once the remanent vector direction is established, a value for the Koenigsberger ratio (Q) and magnetic susceptibility can be determined. In reality, this process provides us with three new parameters because we can also include the probable age of the target.

FIELD EXAMPLES

Two test sites were selected to demonstrate the application of the method to real data. The Black Hill Norite in South Australia has existing rock measurements of magnetic remanence as well as published results for inversion and the magnetic moment method (Schmidt, Clark, and Rajagopalan, 1993, Foss and Mckenzie, 2006). Four isolated anomalies from the Thompson Fold Belt in NSW have been selected to illustrate the method in an under explored region.

Black Hill Norite

Figure 3 shows an image of the total magnetic intensity for a segment of the Black Hill Norite in South Australia. The target remanent magnetic anomaly is located at the image centre. Foss and McKenzie (2006) had previously studied this target using geophysical inversion and two different magnetic moment methods. They used a polygonal shaped plunging prism to allow flexibility with the map geometry of the intrusion.

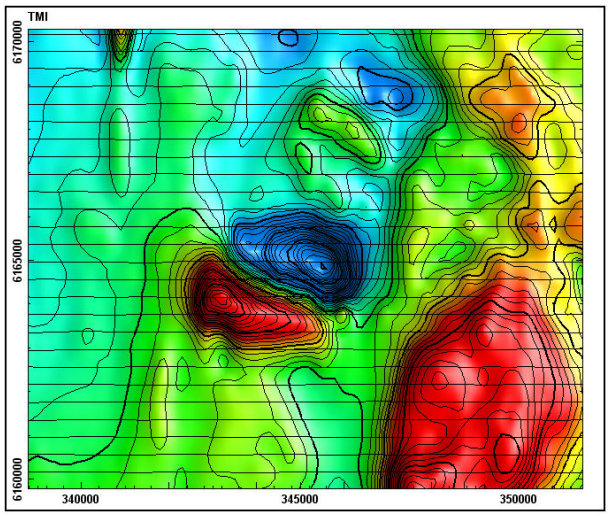

Figure 3. Total magnetic anomaly image of showing the remanently magnetized intrusion of the Black Hill Norite.

We used a simple elliptic prism for the model and the results of the inversion are shown in Figure 4. Regions of the magnetic data that were adversely influenced by cross cutting intrusions were eliminated from the data prior to inversion.

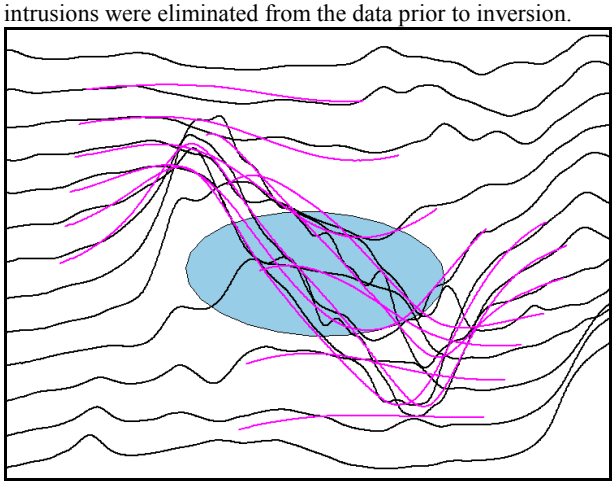

Figure 4. Stacked profile map view of the inversion results (purple), the regional corrected TMI data (black) and the elliptic pipe model outline derived from the inversion.

Table 4 lists the resultant magnetization results from this study and Foss and McKenzie (2006) and the inversion results match within 2 degrees, further boosting the confidence in the robustness of the method. Foss and McKenzie (2006) also report consistent results with different model types used in their inversions. Palaeomagnetic measurements of remanence and our estimates from inversion using the palaeomagnetic pole direction are also shown in Table 4 (bold).

Q values from palaeomagnetic measurements exceed 2 and when we use the average estimate of magnetic susceptibility from Schmidt *et al* (1993) of 0.05 SI, our Q estimate from inversion of the data over the whole intrusion is approximately 5. This is consistent with the very close match between the measured remanent magnetic direction and resultant magnetization direction.

Table 4. Comparison of inversion, magnetic moment and palaeomagnetic rock measurements for the Black Hill Norite.

Source	Method	Dec. (deg)	Inc. (deg)
This study	Res inv	234	9
Foss & McKenzie, 2006	Res inv	232	8
Foss & McKenzie, 2006	MM 1	233	12
Foss & McKenzie, 2006	MM 2	223	6
Rajagapolan *et al*, 1995	Pmag	**221**	**8**
Schmidt *et al*, 1993	Pmag 1	**223**	**9**
Schmidt *et al*, 1993	Pmag 2	**231**	**20**
This study	Rem inv	**230**	**18**

Note: "MM" refers to the magnetic moment method, "Pmag" refers to laboratory palaeomagnetic measurements of rock samples, "Res inv" refers to resultant magnetization vector inversion and "Rem inv" refers to the remanent vector directions derived from inversion using the average laboratory value for magnetic susceptibility.

Schmidt *et al* (1993) used their laboratory measurements to establish a palaeopole location estimate for the Black Hill Norite with an Early Ordovician age of 487 ± 5 million years (Turner, 1990).

Thompson Fold Belt

Figure 5 shows an image of the total magnetic intensity for a segment of the Brewarrina aeromagnetic survey over the southern part of the Thompson Fold Belt (NSW, latitude, 29.84, longitude 147.00). Two negative (A,B) and two positive (C,D) circular anomalies believed to be associated with sub-vertical intrusions have been selected for analysis.

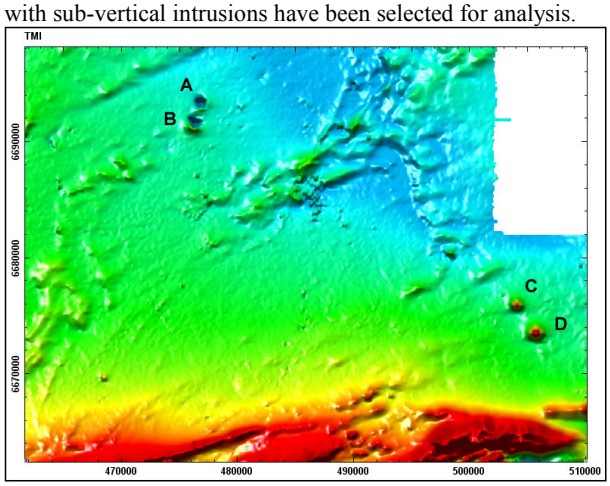

Figure 5. Total magnetic intensity anomaly image of part of the Thompson fold Belt showing four target magnetic anomalies (A, B, C, D).

Targets A and B are strongly reversed with amplitudes of 340 and 400 nanotesla respectively. Targets C and D are normally magnetized with amplitudes of 95 and 120 nT respectively.

Each target was inverted using the original flight line data and the results summarised in Table 5. Target C and D have the appearance of normally magnetized intrusive pipes, yet close inspection using geophysical inversions shows that they have some remanence with ARRA angles of 17.3 and 24.0 respectively. This is well above the limit of sensitivity of the inversion which we expect to be in the range of 2 to 5 degrees for this style of target.

Figure 6 illustrates the methodology used to estimate the magnetic remanence vector direction by displaying the TAPWP trace on a semi-transparent sphere in the vicinity of the remanent vector. The induced field amplitude is modified until the remanent vector intersects the transformed apparent polar wander path.

As a starting point for this research we have used APWP data from Clark and Lackie (2003) and Smith *et al* (2009) which provides data from 15 to 430 million years. Further research is required to provide the best average path with estimates of uncertainties at each step.

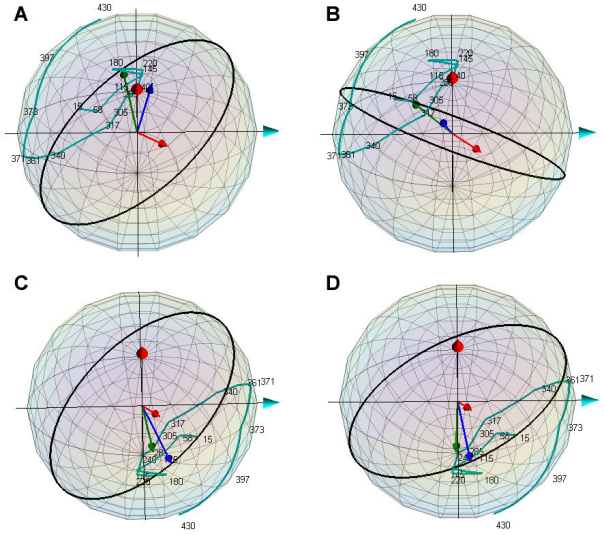

Figure 6. Illustration of the great circle display for each of the targets (A, B, C, D), TAPWP (cyan) traces for the time range 15 to 180 My. The vertical axis arrow (red) shows the north pole and the horizontal axis (cyan) shows the location of the Greenwich meridian. The magnetic vectors are shown in red (induced), blue (resultant) and green (remanent).

Table 5 lists the properties and estimated ages derived by the intersection analysis method. The remanence properties for Targets A and B are similar in magnitude despite the significant shift in declinations and consequently the estimated ages. Targets C and D have much lower magnetic susceptibilities but similar great circles and we note that the TAPWP in Figure 6 has been flipped to the opposite hemisphere to reflect the normal magnetization direction.

Table 5. Comparison of parameters from the inversion results of the four target zones. The inducing field inclination is -61.4 degrees and the declination is 10.1 degrees.

Parameter	**A**	**B**	**C**	**D**
RMS (%)	1.34	0.60	1.57	1.07
Depth (m)	160	115	370	470
Resultant Incl.	60.5	73.0	-74.1	-82.0
Resultant Decl.	63.3	229.6	337.2	321.5
ARRA (deg)	128.5	161.3	17.3	24.0
Remanence Incl.	76	88	-76	-70
Remanence Decl.	120	205	310	224
Susceptibility (SI)	0.224	0.179	0.025	0.022
Q	1.89	1.94	2.05	2.95
Est. age (My)	160	58	160	145

The lower magnetic susceptibilities for pipes C and D could be caused by an equivalence problem as the depth to width ratio is near unity, possibly resulting in an overestimation of diameter and underestimation of the magnetic susceptibility. This issue does not change the remanent magnetization direction or age estimate, but the value of Q could be overestimated.

The apparent age for three of the intrusions is around 145 – 160 million years. The depths for all four intrusions are consistent with the base of the Eromanga Basin sequence which sits over basement rocks of Devonian to Silurian ages. The Jurassic Garawilla Volcanics to the east have an age range of 171 – 208 according to Geoscience Australia's Australian Stratigraphic Names Database and these intrusions are most likely of similar age. Target B has a great circle that is different to the other three targets with an implied younger age of around 58 million years. The estimated separation between the remanence directions for targets A and B is 46 degrees. Given its proximity to A and shallow depth it is probably of similar age to Target A, but the significant implied difference cannot be explained at this time.

CONCLUSIONS

The important outcomes of this research include:

- The ability to detect low level remanent magnetization
- improved target map shape estimation
- estimation of dip in the presence of remanent magnetization
- improved accuracy of magnetic susceptibility estimation
- the ability to estimate the Koenigsberger ratio (Q)
- estimation of the approximate age of the target.

This methodology provides us with a new exploration tool to estimate the remanence properties of buried targets and a diagnostic tool to prioritise target investigation for a range of commodities.

The method is dependent upon the remanent magnetization being relatively unaffected by significant changes with time. These changes are influenced by phenomena such as thermal over-prints, chemical alteration of the single domain and pseudo-single domain magnetic carriers and the onset of viscous or isothermal remanent magnetization effects in the original source rocks (Clark, 1997). The principle of establishing the intersection of the TAPWP with the great circle will however, provide many useful outcomes for explorers as they begin to look at ways to use this new method for the remote determination of magnetic remanence.

ACKNOWLEDGMENTS

Encom ModelVision from Pitney Bowes Business Insight was used to perform the magnetic inversions for both the research and field applications. Encom PA Professional was used for the generation of the image displays.

The authors would like to thank Phil Schmidt, Clive Foss (CSIRO) and Robert Musgrave (NSW Geological Survey) for their helpful input on magnetic polar wander data and the magnetic moment methods.

REFERENCES

Caratori Tontini, F. and Pedersen, L.B., 2008. Interpretating magnetic data using integral moments: *Geophysical Journal International*, **174**, 815-824.

Clark, D.A., 1997. Magnetic petrophysics and magnetic petrology: aids to geological interpretation of magnetic surveys: *AGSO Journal of Australian Geology and Geophysics* **17(2)**, 83-103.

Clark, D.A. and Lackie, M.A., 2003. Palaeomagnetism of the Early Permain Mount Leyshon Intrusive Complex and the Tuckers Igneous Complex, North Queensland, Australia: *Geophysical Journal International*, **153**, 523-547.

Cordani, R. and Shukowsy, W., 2009. Virtual Pole from magnetic Anomaly (VPMA): A procedure to estimate the age of a rock from its magnetic anomaly only: *Journal of Applied Geophysics*, **69**, 96-102.

Foss, C.A. and McKenzie, K.B., 2006, Inversion of anomalies due to remanent magnetization – an example from the Black Hill Norite of South Australia: *ASEG Extended Abstracts AESC2006, Melbourne, Australia*.

McKenzie, K.B, Hillan, D. and Foss, C.A., 2012, An improved search for magnetization direction: *In Press, Extended Abstracts, ASEG 22nd International Conference and Exhibition, Brisbane*.

Grant F.S. and West, G.F., 1965, *Interpretation Theory in Applied Geophysics*: McGraw-Hill, New York.

Merrill, R.T., McElhinny, W. and McFadden, P.L., 1996. *The Magnetic Field of the Earth*: Academic Press.

Rajagopalan, S., Clark, D.A. and Schmidt, P.W., 1995, Magnetic mineralogy of the Black Hill Norite and its aeromagnetic and palaeomagnetic implications: *Exploration Geophysics*, **26**, 215-220.

Schmidt, P.W., Clark, D.A. and Rajagopalan, S. 1993, An historical perspective of the Early Palaeozoic APWP of Gondwana: New results from the Early Ordovician Black Hill Norite of South Australia: *Exploration Geophysics,* **24**, 257-262.

Schmidt, P.W., and Clark, D.A., 1998, The calculation of magnetic components and moments from TMI: A case study from the Tuckers igneous complex, Queensland: *Exploration Geophysics*, **29**, 609-614.

Smith, M.L., Pillans, B.J. and McQueen, K.G., 2009, Paleomagnetic evidence for periods of intense oxidation weathering, McKinnons mine, Cobar, New South Wales: *Australian Journal of Earth Sciences*, **56**, 201-212.

Turner, S.P., 1991, 'Late-orogenic, mantle-derived, bi-modal magmatism in the southern Adelaide Foldbelt, South Australia': *Ph.D. Thesis (unpubl), University of Adelaide*.